Five Steps for Creating an Original Figure for a Poster

Brian H. Lower (Ph.D.)

SOME THINGS TO CONSIDER BEFORE YOU BEGIN:

You should start designing your poster by creating a **Poster Outline** of what you will include in your poster and where you want it to appear in your poster.

Decide what figures and/or tables you want to include in your poster and where these will go.

Well designed posters typically have 6-8 figures or tables that take up the majority of the space on the poster. A poster contains **minimal text because the figures should "tell the story" to the audience**.

A figure can be a graph, diagram, photograph, illustration, flowchart, map, histogram, image, etc.

Create the figures for your poster using Microsoft PowerPoint, Microsoft Excel, Apple Keynote, Apple Numbers or Photoshop.

Make sure to use **high resolution figures** in your poster because your final poster will be much larger than a typical sheet of paper. Your poster will be 36-inches (height) by 48-inches (width).

Step 1: Download the journal article (PDF file) from Web of Science

Reference Information:

Authors: Louf, J-F., L. Nelson, H. Kang, P. N. Song, T. Zehnbauer, S. Jung

Article Title: How wind drives the correlation between leaf shape and mechanical properties

Publication Year: 2018

Journal: Scientific Reports

Volume: 8

Pages: e15314 (1-6)

Type of Publication: Primary Source

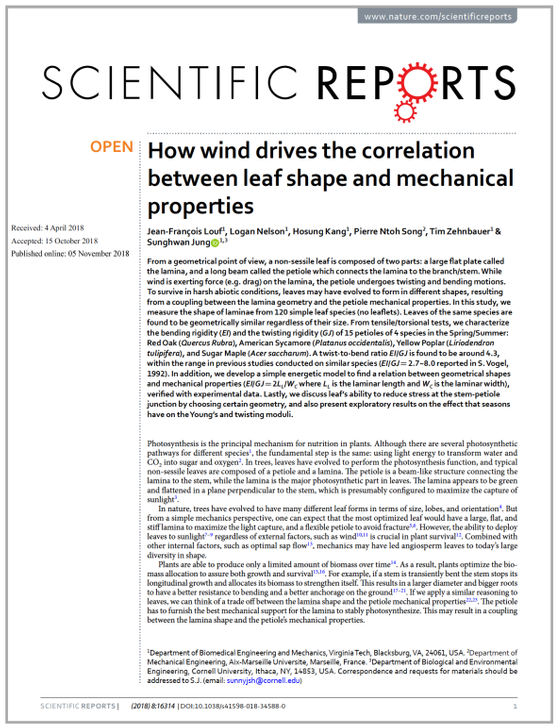
www.nature.com/scientificreports

SCIENTIFIC REPORTS

OPEN

How wind drives the correlation between leaf shape and mechanical properties

Jean-François Louf[1], Logan Nelson[1], Hosung Kang[1], Pierre Ntoh Song[2], Tim Zehnbauer[1] & Sunghwan Jung[1,3]

Received: 4 April 2018
Accepted: 15 October 2018
Published online: 05 November 2018

From a geometrical point of view, a non-sessile leaf is composed of two parts: a large flat plate called the lamina, and a long beam called the petiole which connects the lamina to the branch/stem. While wind is exerting force (e.g. drag) on the lamina, the petiole undergoes twisting and bending motions. To survive in harsh abiotic conditions, leaves may have evolved to form in different shapes, resulting from a coupling between the lamina geometry and the petiole mechanical properties. In this study, we measure the shape of laminae from 120 simple leaf species (no leaflets). Leaves of the same species are found to be geometrically similar regardless of their size. From tensile/torsional tests, we characterize the bending rigidity (*EI*) and the twisting rigidity (*GJ*) of 15 petioles of 4 species in the Spring/Summer: Red Oak (*Quercus Rubra*), American Sycamore (*Platanus occidentalis*), Yellow Poplar (*Liriodendron tulipifera*), and Sugar Maple (*Acer saccharum*). A twist-to-bend ratio *EI*/*GJ* = 2.7–8.0 reported in S. Vogel, 1992). In addition, we develop a simple energetic model to find a relation between geometrical shapes and mechanical properties (*EI*/*GJ* ≈ 2*L*$_l$/*W*$_l$, where *L*$_l$ is the laminar length and *W*$_l$ is the laminar width), verified with experimental data. Lastly, we discuss leaf's ability to reduce stress at the stem-petiole junction by choosing certain geometry, and also present exploratory results on the effect that seasons have on the Young's and twisting moduli.

Photosynthesis is the principal mechanism for nutrition in plants. Although there are several photosynthetic pathways for different species[1], the fundamental step is the same: using light energy to transform water and CO_2 into sugar and oxygen[2]. In trees, leaves have evolved to perform the photosynthesis function, and typical non-sessile leaves are composed of a petiole and a lamina. The petiole is a beam-like structure connecting the lamina to the stem, while the lamina is the major photosynthetic part in leaves. The lamina appears to be green and flattened in a plane perpendicular to the stem, which is presumably configured to maximize the capture of sunlight[3].

In nature, trees have evolved to have many different leaf forms in terms of size, lobes, and orientation[4]. But from a simple mechanics perspective, one can expect that the most optimized leaf would have a large, flat, and stiff lamina to maximize the light capture, and a flexible petiole to avoid fracture[5,6]. However, the ability to deploy leaves to sunlight[7–9] regardless of external factors, such as wind[10,11] is crucial in plant survival[12]. Combined with other internal factors, such as optimal sap flow[13], mechanics may have led angiosperm leaves to today's large diversity in shape.

Plants are able to produce only a limited amount of biomass over time[14]. As a result, plants optimize the biomass allocation to assure both growth and survival[15,16]. For example, if a stem is transiently bent the stem stops its longitudinal growth and allocates its biomass to strengthen itself. This results in a larger diameter and bigger roots to have a better resistance to bending and a better anchorage on the ground[17–21]. If we apply a similar reasoning to leaves, we can think of a trade off between the lamina shape and the petiole mechanical properties[22,23]. The petiole has to furnish the best mechanical support for the lamina to stably photosynthesize. This may result in a coupling between the lamina shape and the petiole's mechanical properties.

[1]Department of Biomedical Engineering and Mechanics, VirginiaTech, Blacksburg, VA, 24061, USA. [2]Department of Mechanical Engineering, Aix-Marseille Universite, Marseille, France. [3]Department of Biological and Environmental Engineering, Cornell University, Ithaca, NY, 14853, USA. Correspondence and requests for materials should be addressed to S.J. (email: sunnyjsh@cornell.edu)

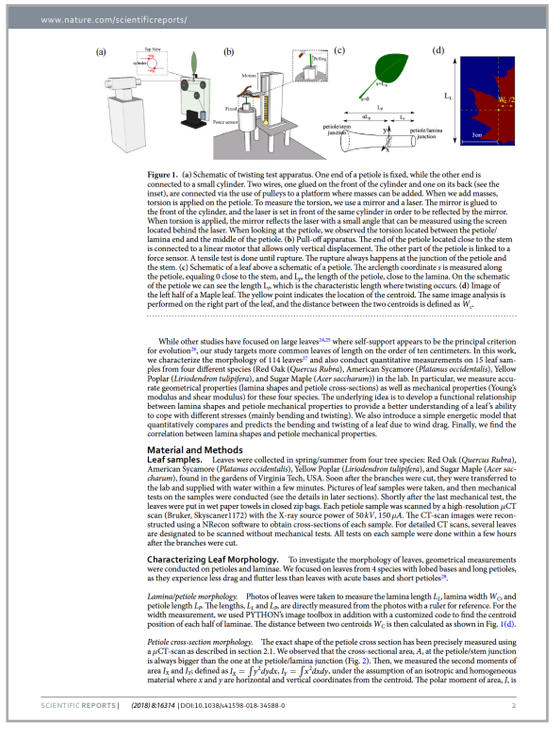

Figure 1. (**a**) Schematic of twisting test apparatus. One end of a petiole is fixed, while the other end is connected to a small cylinder. Two wires, one glued on the front of the cylinder and one on its back (see the inset), are connected via the use of pulleys to a platform where masses can be added. When we add masses, torsion is applied on the petiole. To measure the torsion, we use a mirror and a laser. The mirror is glued to the front of the cylinder, and the laser is set in front of the same cylinder in order to be reflected by the mirror. When torsion is applied, the mirror reflects the laser with a small angle that can be measured using the screen located behind the laser. When looking at the petiole, we observed the torsion located between the petiole/lamina end and the middle of the petiole. (**b**) Pull-off apparatus. The end of the petiole located close to the stem is connected to a linear motor that allows only vertical displacement. The other part of the petiole is linked to a force sensor. A tensile test is done until rupture. The rupture always happens at the junction of the petiole and the stem. (**c**) Schematic of a leaf above a schematic of a petiole. The arclength coordinate s is measured along the petiole, equaling 0 close to the stem, and L_p, the length of the petiole, close to the lamina. On the schematic of the petiole we can see the length L_n which is the characteristic length where twisting occurs. (**d**) Image of the left half of a Maple leaf. The yellow point indicates the location of the centroid. The same image analysis is performed on the right part of the leaf, and the distance between the two centroids is defined as W_c.

While other studies have focused on large leaves[24,25] where self-support appears to be the principal criterion for evolution[26], our study targets more common leaves of length on the order of ten centimeters. In this work, we characterize the morphology of 114 leaves[27] and also conduct quantitative measurements on 15 leaf samples from four different species (Red Oak (*Quercus Rubra*), American Sycamore (*Platanus occidentalis*), Yellow Poplar (*Liriodendron tulipifera*), and Sugar Maple (*Acer saccharum*)) in the lab. In particular, we measure accurate geometrical properties (lamina shapes and petiole cross-sections) as well as mechanical properties (Young's modulus and shear modulus) for these four species. The underlying idea is to develop a functional relationship between lamina shapes and petiole mechanical properties to provide a better understanding of a leaf's ability to cope with different stresses (mainly bending and twisting). We also introduce a simple energetic model that quantitatively compares and predicts the bending and twisting of a leaf due to wind drag. Finally, we find the correlation between lamina shapes and petiole mechanical properties.

Material and Methods

Leaf samples. Leaves were collected in spring/summer from four tree species: Red Oak (*Quercus Rubra*), American Sycamore (*Platanus occidentalis*), Yellow Poplar (*Liriodendron tulipifera*), and Sugar Maple (*Acer saccharum*), found in the gardens of Virginia Tech, USA. Soon after the branches were cut, they were transferred to the lab and supplied with water within a few minutes. Pictures of leaf samples were taken, and then mechanical tests on the samples were conducted (see the details in later sections). Shortly after the last mechanical test, the leaves were put in wet paper towels in closed zip bags. Each petiole sample was scanned by a high-resolution μCT scan (Bruker, Skyscan1172) with the X-ray source power of 50 kV, 150 μA. The CT-scan images were reconstructed using a NRecon software to obtain cross-sections of each sample. For detailed CT scans, several leaves are designated to be scanned without mechanical tests. All tests on each sample were done within a few hours after the branches were cut.

Characterizing Leaf Morphology. To investigate the morphology of leaves, geometrical measurements were conducted on petioles and laminae. We focused on leaves from 4 species with lobed bases and long petioles, as they experience less drag and flutter less than leaves with acute bases and short petioles[28].

Lamina/petiole morphology. Photos of leaves were taken to measure the lamina length L_l, lamina width W_l, and petiole length L_p. The lengths, L_l and L_p, are directly measured from the photos with a ruler for reference. For the width measurement, we used PYTHON's image toolbox in addition with a customized code to find the centroid position of each half of laminae. The distance between two centroids W_c is then calculated as shown in Fig. 1(d).

Petiole cross-section morphology. The exact shape of the petiole cross section has been precisely measured using a μCT-scan as described in section 2.1. We observed that the cross-sectional area, A, at the petiole/stem junction is always bigger than the one at the petiole/lamina junction (Fig. 2). Then, we measured the second moments of area I_x and I_y defined as $I_x = \int y^2 dydz$, $I_y = \int x^2 dydy$, under the assumption of an isotropic and homogeneous material where x and y are horizontal and vertical coordinates from the centroid. The polar moment of area, J, is

Figure 2. Pictures of the leaves of the four species studied, from left to right: (**a**) Red Oak, (**b**) American Sycamore, (**c**) Yellow Poplar, and (**d**) Sugar Maple. Under each picture there is a plot of the area A and the polar moment of Inertia J along the petiole. An exponential fit done on J (in black) allows us to calculate $\alpha \times L_p$ corresponding at the location where J is decreased by 99%. This coefficient α is then used to accurately determine the twisting length $L_t = (1-\alpha)L_p$.

defined as the sum of the two second moments of area I_x and I_y. We were thus able to obtain I_x, I_y, and J everywhere along the petiole. All values calculated using the μCT-scan are an average of 50 representative images (1.1–1.4 mm along the axial direction).

Mechanical Properties. To understand the twisting and bending motions, torsional and tensile tests have been conducted on petioles.

Twisting length. Niklas *et al.*[29] have shown that there are two types of petioles: one with uniform cross-sectional area and stiffness (EI), and one which is tapered with a basipetal increase of the stiffness. For the latter case, twisting does not occur uniformly along the petiole, but rather develops more in the portion of smaller second moment of area. As a result, in our twisting experiment, to accurately measure GJ we need to know what the characteristic twisting length is. With measured A and J, we fit J with an exponential function and calculate the 99th percentile of its maximum value (Fig. 2). Then, the distance from this point to the lamina is defined as our twisting length L_t (Fig. 1(c)), which will be used in the calculation of GJ.

Torsional test. A new experimental set-up inspired by Vogel[30] has been designed (Fig. 1(a)), which allows us to precisely measure the global torsional rigidity GJ. The petiole/lamina junction was fixed on an upper holder, and the other end (petiole/stem junction) was clamped on a lower cylinder. On the front and back sides of the cylinder, two wires were attached and linked to pulleys, which are fixed onto a platform with a weight. By changing the weight, we were able to control the torsional force applied to the petiole. To measure this torsional angle, a mirror was attached on the cylinder with a laser pointed at it. When torsion is applied, the cylinder rotates and then reflects the laser light in a different direction. Using this method, we can translate and amplify the small rotational motion to the large linear displacement of the laser on a white screen. By measuring the distance between the initial and final positions of the laser on the screen, we were able to back-calculate the deflection angle, and thereby the rotational deformation. The accuracy of our set-up was confirmed by conducting a few test experiments on cylindrical bars of elastomer (ZhermackDouble Elite 8, and 22), whose Young's moduli were measured using an Instron machine (E = 0.2 and 0.9 MPa, respectively). Assuming that the polymer has a Poisson's ratio of 1/2, we obtain the following relation between the twisting and Young moduli: $G = E/3$. We found the difference between the experimental tests and the expected values to be less than 5%.

Tensile test. The next mechanical test is an experiment in which leaves are pulled as shown in Fig. 1(b). The tensile tests were conducted on petioles in order to measure the traction Young's modulus. The lamina end of the petiole was squeezed and fixed on a force sensor (LCM105-10, Omegadyne, Inc.), while the stem end was fixed to a linear stage (see the inset of Fig. 1(b)). A constant pulling speed of 1.27 mm/s was applied, and the force acting on the petiole was recorded from the sensor. Tests were performed to failure of the petiole, which always occurred at the petiole/stem junction. The stress was calculated after measuring the petiole cross section at the junction where it failed, and the strain was measured from the displacement of the linear stage. Finally, we plotted a stress-strain curve, giving us the Young's modulus E of the petiole.

Results

When subjected to wind, a long slim lamina will induce more bending stress to its petiole than shearing stress. In contrast, a short wide lamina will produce more shearing stress associated with twisting motions than bending stress to its petiole. In order to be compliant with either twisting or bending forces resulting from its lamina shape, the petiole presumably has an optimized shape and mechanical properties. In this study, we characterized the

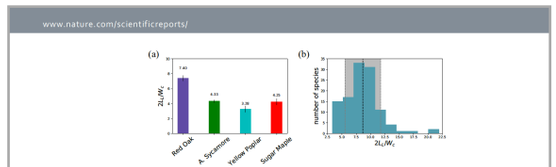

Figure 3. (**a**) Ratio of two times the lamina and the width between the centroids, for the four species tested in the lab. The small error bars indicate that leaves among a species are homothetic, as assumed by an existing model[24]. (**b**) Ratio of two times the lamina and the width between the centroids, for 114 leaves[27]. The complete list of the species and the corresponding value for their ratio is given in Appendix A. The average indicated by the black line is 8.7, and the grey area represents the plus or minus one standard deviation (3.1).

Young's modulus E (Pa), the shear modulus G (Pa), the second moment of area I_x (m^4), and the polar moment of area J (m^4), and checked for correlations with lamina shape.

Flexural stiffness ratio. Using data obtained from the morphology measurements and mechanical tests, we were able to access the flexural rigidity EI_x. The variable I_x is calculated in the circular part of the petiole (local quantity). The flexural rigidity quantifies the resistance of a leaf to pull-off after bending, and the twisting rigidity quantifies its resistance to twist-off. These two quantities can be used to calculate the flexural stiffness ratio EI_x/GJ defined by Vogel[30]. Moreover, by writing a simple force balance between the twisting and bending of a leaf resulting from the action of the wind, we can also write a more accurate scaling law.

The drag M_{drag} (N·m) exerted by wind on a lamina scales as

$$M_{drag} \approx \frac{1}{2}\rho U^2 L_l W_c \frac{L_l}{2} \tag{1}$$

	2009	2010	2011	2012	2013	2014	2015	2016	2017	2018
American Sycamore	131	136	134	140	142	146	148	146	150	152
Red Maple	123	120	104	100	95	80	63	55	51	50
Tulip Poplar	235	238	243	269	286	312	342	373	403	433
White Oak	429	415	401	365	302	286	222	150	73	51
Total	918	909	882	874	847	824	775	724	677	686

Similarly, we can write torque T_{drag} (N·m) resulting from the drag as

$$T_{drag} \approx \frac{1}{2}\rho U^2 L_l \frac{W_c}{2}\frac{W_c}{2}, \tag{3}$$

and the associated twisting angle Θ^{twist} is given as

$$\Theta^{twist} = \frac{T_{drag} L_p}{GJ}. \tag{4}$$

These two angles can be used to estimate the projected areas of the leaf to the vertical axis (towards the sun) due to bending and twisting motions, respectively. Here, the projected areas are the product of the cosine of the angles and the original lamina area A_l. In order to improve the amount of direct sunlight, a leaf might have the same ratio of projected areas due to bending and twisting[31]. Under this hypothesis, both angles should be equal as

$$\frac{L_p}{EI_x}\left(\frac{1}{2}\rho U^2 L_l W_c \frac{L_l}{2}\right) = \frac{L_p}{GJ}\left[\frac{1}{2}\rho U^2 L_l \frac{W_c^2}{4}\right] \tag{5}$$

If we assume that the projected area is large to maximize photosynthesis, then we can write $A_p^{bend} = A_p^{twist}$ which leads to:

$$EI_x \approx \frac{2L_l}{W_c} GJ \tag{6}$$

In our case, the ratio $2L_l/W_c$ is found to be in the range 3–8 for species studied in the lab (see Fig. 3(a)). Here, we find that the variation among a species is very small and that each species has a different ratio (Kruskal-Wallis H-test p-value is less than 0.009), meaning that leaves of a single species are both geometrically and statistically similar (in the same shape, but of different sizes).

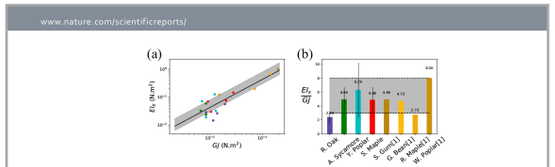

Figure 4. (**a**) Log-log plot of EI_x as a function of GJ for 8 different species. The coefficient of linear correlation r between EI_x and GJ for our data is 0.6, with 15 samples, meaning that we have at least a 93% probability that our data are indeed linearly correlated[32]. The black line is the best fit coefficient 4.3 obtained from only our experimental data - data from the literature[30] were later added on top. The gray area illustrates the prediction of our model based on the species we studied. (**b**) Ratio of EI_x vs GJ for our species and species from Vogel[30]. The gray area indicates the prediction from our model based on the leaf shapes tested in the lab.

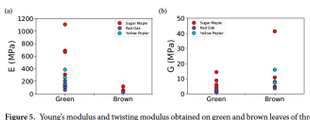

Figure 5. Young's modulus and twisting modulus obtained on green and brown leaves of three different species. (**a**) The Young's modulus of brown leaves is drastically lower than the Young's modulus of green leaves. However, (**b**) the twisting moduli of green and brown leaves are not statistically different.

Moreover, we analyzed 114 more lamina shapes[27] to extend the number of the data set of $2L_l/W_c$ (Fig. 3(b)). We obtain an average value of $2L_l/W_c = 8.7 \pm 3.1$ which is a bit higher than our lab measurements because of a few outliers (Black Cherry, Corkscrew Willow, Shingle Oak, and White Willow).

To validate our linear relationship of Eq. 6, we plot EI_x as a function of GJ as shown in Fig. 4(a). We can see that, as predicted by our model, EI_x linearly increases with GJ. The coefficient of linear correlation r, quantifying if data are linearly correlated or not, is 0.6, with 15 samples. This result means that we have at least a 93% probability that our data are indeed linearly correlated[32]. The average slope of our lab data is 4.3. This is in agreement with Vogel's data[30] which was later on added on the plot. We experimentally find that the ratio EI_x/GJ of both our data and Vogel's data[30] is approximately in a range between 3 and 8. In Fig. 4(b), we plot the ratio EI_x/GJ for each species and the experimental ratio $2L_l/W_c$ as a gray-shaded region. This plot indicates that these two ratios (EI_x/GJ & $2L_l/W_c$) are in the same range, showing the validity and robustness of our model.

Discussion and Conclusion

In this study, we elucidated the relation between the lamina shapes and the petiole mechanical properties through a series of experiments. First, both torsional and tensional tests were performed to evaluate the bending and twisting rigidities of petioles. Second, μ-CT scanned images allowed us to estimate the second moment of inertia and cross-sectional area along petioles. Third, both width and length of laminae were measured from images. As a result, we found that among a species the shape of leaves is geometrically similar. Lastly, using mechanical testing performed on leaves in the lab, we showed that it is energetically easier for a leaf to twist than to bend, and furthermore, the famous Vogel's twist-to-bend ratio is linked to the shape of the laminae. However, it is worth noting the limit of our model: statistically the ratio EI_x/GJ does not differ between the four different species tested (Kruskal-Wallis H-test gives a p-value of 0.33), preventing us to draw any correlation between the mechanical and geometrical properties of leaves *per species*.

As we described in section 3, twisting mainly occurs in a portion of the petiole close to the lamina, but the twisting length, L_t, depends on the species. Mechanically, flexural rigidity and torsional rigidity are composite variables that are influenced both by material and structural properties[33]. However, by just altering geometrical properties, petioles succeeded in changing the location of the twisting area closer to the lamina. With such a geometry, even if the stress is constant throughout the petiole, the strain is smaller close to the stem.

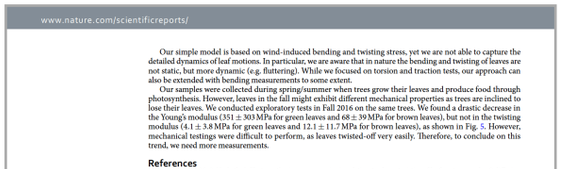

Our simple model is based on wind-induced bending and twisting stress, yet we are not able to capture the detailed dynamics of leaf motions. In particular, we are aware that in nature the bending and twisting of leaves are not static, but more dynamic (e.g. fluttering). While we focused on torsion and traction tests, our approach can also be extended with bending measurements to some extent.

Our samples were collected during spring/summer when trees grow their leaves and produce food through photosynthesis. However, leaves in the fall might exhibit different mechanical properties as trees are inclined to lose their leaves. We conducted exploratory tests in Fall 2016 on the same trees. We found a drastic decrease in the Young's modulus (351 ± 303 MPa for green leaves and 68 ± 39 MPa for brown leaves), but not in the twisting modulus (4.1 ± 3.8 MPa for green leaves and 12.1 ± 11.7 MPa for brown leaves), as shown in Fig. 5. However, mechanical testings were difficult to perform, as leaves twisted-off very easily. Therefore, to conclude on this trend, we need more measurements.

References

1. El-Sharkawy, M. & Hesketh, J. Photosynthesis among species in relation to characteristics of leaf anatomy and co2 diffusion resistances. *Crop. Sci.* **5**, 517–521 (1965).
2. Vogel, S. The life of a leaf (University of Chicago Press, Chicago, 2012).
3. Tadrist, L., Saudreau, M. & de Langre, E. Wind and gravity mechanical effects on leaf inclination angles. *J. Theor. Biol.* **341**, 9–16 (2014).
4. Niklas, K. J. Plant Allometry (University of Chicago Press, 1994).
5. Niklas, K. Plant biomechanics: an engineering approach to plant form and function (The University of Chicago Press, 1992).
6. Niinemets, Ü. & Fleck, S. Petiole mechanics, leaf inclination, morphology, and investment in support in relation to light availability in the canopy of liriodendron tulipifera. *Oecologia* **132**, 21–33 (2002).
7. Roden, J. S. & Pearcy, R. W. Effect of leaf flutter on the light environment of poplars. *Oecologia* **93**, 201–207 (1993).
8. Takemaka, A. Effects of leaf blade narrowness and petiole length on the light capture efficiency of a shoot. *Ecol. Res.* **9**, 109–114 (1994).
9. Roden, J. S. Modeling the light interception and carbon gain of individual fluttering aspen (populus tremuloides michx) leaves. *Trees* **17**, 117–126 (2003).
10. Vogel, S. Leaves in the lowest and highest winds: temperature, force and shape. *New Phytol.* **183**, 13–26 (2009).
11. Anten, N. P. R., Alcalá-Herrera, R., Schieving, F. & Onoda, Y. Wind and mechanical stimuli differentially affect leaf traits in plantago major. *New Phytol.* **188**, 554–564 (2010).
12. de Langre, E. Effects of wind on plants. *Annu. Rev. Fluid Mech.* **40**, 141–168 (2008).
13. Jensen, K. H. & Zwieniecki, M. A. Physical limits to leaf size in tall trees. *Phys. Rev. Lett.* **110**, 018104 (2013).
14. Poorter, H. & Nagel, O. The role of biomass allocation in the growth response of plants to different levels of light, co2, nutrients and water: a quantitative review. *Aust. J. Plant Physiol.* **27**, 595–607 (2000).
15. Niklas, K. J. Biomechanical responses of chamaedorea and spathiphyllum petioles to tissue dehydration. *Annals Bot.* **67**, 67–76 (1991).
16. Duan, S. *et al.* The global spectrum of plant form and function. *Nat.* **529**, 167–171 (2015).
17. Jaffe, M. J. T. The response of plant growth and development to mechanical stimulation. *Planta* **114**, 143–157 (1973).
18. Knight, T. A. Account of some experiments on the descent of sap in trees. Philos. *Transactions Royal Soc. Lond.* **93**, 277–289 (1803).
19. Jacobs, M. R. The effect of wind sway on the form and development of pinus radiata d. don. *Aust. J. Bot.* **2**(2), 35–51 (1954).
20. Coutand, C. Biomechanical study of the effect of a controlled bending on tomato stem elongation: global mechanical analysis. *J. Exp. Bot.* **51**, 1813–1824 (2000).
21. Loué, J., Guena, G., Badel, E. & Forterre, Y. A universal mechanism for hydraulic signals generation in biomimetic and natural branches. *Proc. Natl. Acad. Sci.* **114**, 11034–11039 (2017).
22. Niklas, K. J. The elastic moduli and mechanics of populus tremuloides (salicaceae) petioles in bending and torsion. *Am. J. Bot.* **78**, 989–996 (1991).
23. Niklas, K. J. Differences between acer saccharum leaves from open and wind-protected sites. *Annals Bot.* **78**, 61–66 (1996).
24. Ennos, A. R., Spatz, H. & Speck, T. The functional morphology of the petioles of the banana, Musa textilis. *J. Exp. Bot.* **51**, 2085–2093 (2000).
25. Hejnowicz, Z. & Barthlott, W. Structural and mechanical peculiarities of the petioles of giant leaves of amorphophallus (araceae). *Am. J. Bot.* **82**, 391–403 (2005).
26. Tadrist, L. & Barbosa-Tessier, B. Are leaves optimally designed for self-support? an investigation on giant monocots. *J. Theor. Biol.* **396**, 125–131 (2016).
27. Chang, Y.-W. *et al.* Leafsnap: An electronic field guide (2011).
28. Vogel, S. Drag and reconfiguration of broad leaves in high winds. *J. Exp. Bot.* **40**, 941–948 (1989).
29. Niklas, K. J. Flexural stiffness allometry of angiosperm and fern petioles and rachises: evidence for biomechanical convergence. *Evol.* **45**, 734–750 (1991).
30. Vogel, S. Twist-to-bend ratios and cross-sectional shapes of petioles and stems. *J. Exp. Bot.* **43**, 1527–1532 (1992).
31. Monsi, M. & Saeki, T. On the factor light in plant communities and its importance for matter production. *Annals Bot.* **95**, 549–567 (2005).
32. Taylor, J. R. An Introduction to Error Analysis (University Science Books, 1982).
33. Wainwright, S. A., Biggs, W. D., Currey, J. D. & Gosline, J. M. Mechanical Design in Organism (Princeton University Press, Princeton, 1976).
34. Toselli, F. & Bodechtel, J. Imaging Spectroscopy: Fundamentals and Prospective Applications (Kluwer Academic Publishers, 1991).

Acknowledgements

This research was supported by National Science Foundation Grant CBET-1604424. Hosung Kang was supported by the Postdoctoral Research Program of Sungkyunkwan University (2015).

Author Contributions

J.-F.L., P.N.S., T.Z. and S.J. designed research; J.-F.L., L.N., H.K., P.N.S., T.Z. and S.J. performed research; J.-F.L., L.N., P.N.S., T.Z. and S.J. analyzed data; and J-F.L., T.Z. and S.J. wrote the paper.

Additional Information

Supplementary information accompanies this paper at https://doi.org/10.1038/s41598-018-34588-0.

Competing Interests: The authors declare no competing interests.

Step 2: Determine what information (or data) you would like to take from the journal article and use in your poster.

Citation: Louf, J-F., L. Nelson, H. Kang, P. N. Song, T. Zehnbauer, S. Jung (2018). Scientific Reports, 8:15314.

I want to put data from this table into my poster

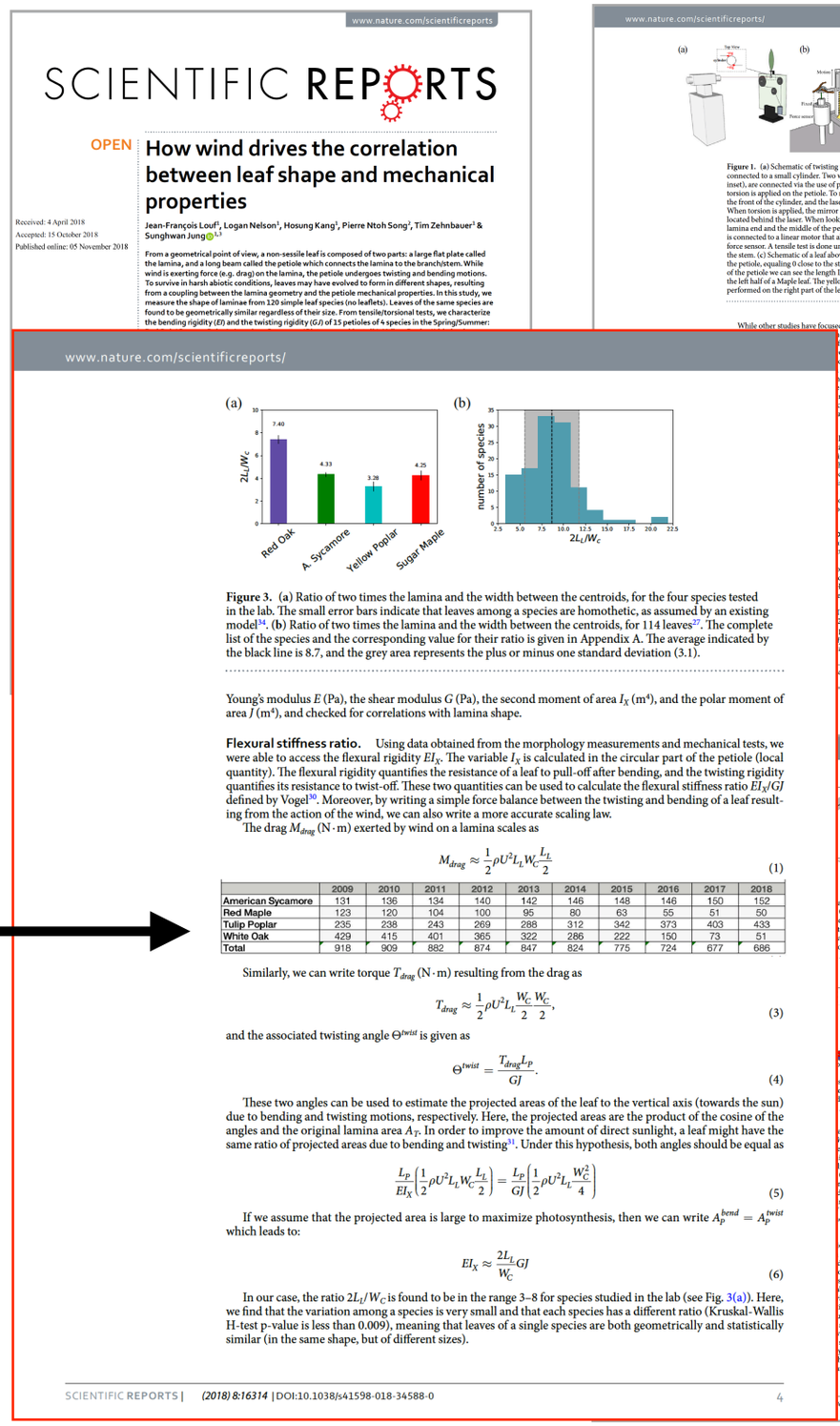

www.nature.com/scientificreports

SCIENTIFIC REPORTS

OPEN

How wind drives the correlation between leaf shape and mechanical properties

Jean-François Louf[1], Logan Nelson[1], Hosung Kang[1], Pierre Ntoh Song[2], Tim Zehnbauer[1] & Sunghwan Jung[1,3]

Received: 4 April 2018
Accepted: 15 October 2018
Published online: 05 November 2018

From a geometrical point of view, a non-sessile leaf is composed of two parts: a large flat plate called the lamina, and a long beam called the petiole which connects the lamina to the branch/stem. While wind is exerting force (e.g. drag) on the lamina, the petiole undergoes twisting and bending motions. To survive in harsh abiotic conditions, leaves may have evolved to form in different shapes, resulting from a coupling between the lamina geometry and the petiole mechanical properties. In this study, we measure the shape of laminae from 120 simple leaf species (no leaflets). Leaves of the same species are found to be geometrically similar regardless of their size. From tensile/torsional tests, we characterize the bending rigidity (EI) and the twisting rigidity (GJ) of 15 petioles of 4 species in the Spring/Summer:

www.nature.com/scientificreports/

Figure 3. (a) Ratio of two times the lamina and the width between the centroids, for the four species tested in the lab. The small error bars indicate that leaves among a species are homothetic, as assumed by an existing model[34]. (b) Ratio of two times the lamina and the width between the centroids, for 114 leaves[27]. The complete list of the species and the corresponding value for their ratio is given in Appendix A. The average indicated by the black line is 8.7, and the grey area represents the plus or minus one standard deviation (3.1).

Young's modulus E (Pa), the shear modulus G (Pa), the second moment of area I_X (m⁴), and the polar moment of area J (m⁴), and checked for correlations with lamina shape.

Flexural stiffness ratio. Using data obtained from the morphology measurements and mechanical tests, we were able to access the flexural rigidity EI_X. The variable I_X is calculated in the circular part of the petiole (local quantity). The flexural rigidity quantifies the resistance of a leaf to pull-off after bending, and the twisting rigidity quantifies its resistance to twist-off. These two quantities can be used to calculate the flexural stiffness ratio EI_X/GJ defined by Vogel[30]. Moreover, by writing a simple force balance between the twisting and bending of a leaf resulting from the action of the wind, we can also write a more accurate scaling law.

The drag M_{drag} (N·m) exerted by wind on a lamina scales as

$$M_{drag} \approx \frac{1}{2}\rho U^2 L_L W_C \frac{I_L}{2} \tag{1}$$

	2009	2010	2011	2012	2013	2014	2015	2016	2017	2018
American Sycamore	131	136	134	140	142	146	148	146	150	152
Red Maple	123	120	104	100	95	80	63	55	51	50
Tulip Poplar	235	238	243	269	288	312	342	373	403	433
White Oak	429	415	401	365	322	286	222	150	73	51
Total	918	909	882	874	847	824	775	724	677	686

Similarly, we can write torque T_{drag} (N·m) resulting from the drag as

$$T_{drag} \approx \frac{1}{2}\rho U^2 L_L \frac{W_C}{2}\frac{W_C}{2}, \tag{3}$$

and the associated twisting angle Θ^{twist} is given as

$$\Theta^{twist} = \frac{T_{drag} L_P}{GJ}. \tag{4}$$

These two angles can be used to estimate the projected areas of the leaf to the vertical axis (towards the sun) due to bending and twisting motions, respectively. Here, the projected areas are the product of the cosine of the angles and the original lamina area A_T. In order to improve the amount of direct sunlight, a leaf might have the same ratio of projected areas due to bending and twisting[31]. Under this hypothesis, both angles should be equal as

$$\frac{L_P}{EI_X}\left(\frac{1}{2}\rho U^2 L_L W_C \frac{L_L}{2}\right) = \frac{L_P}{GJ}\left(\frac{1}{2}\rho U^2 L_L \frac{W_C^2}{4}\right) \tag{5}$$

If we assume that the projected area is large to maximize photosynthesis, then we can write $A_P^{bend} = A_P^{twist}$ which leads to:

$$EI_X \approx \frac{2L_L}{W_C} GJ \tag{6}$$

In our case, the ratio $2L_l/W_C$ is found to be in the range 3–8 for species studied in the lab (see Fig. 3(a)). Here, we find that the variation among a species is very small and that each species has a different ratio (Kruskal-Wallis H-test p-value is less than 0.009), meaning that leaves of a single species are both geometrically and statistically similar (in the same shape, but of different sizes).

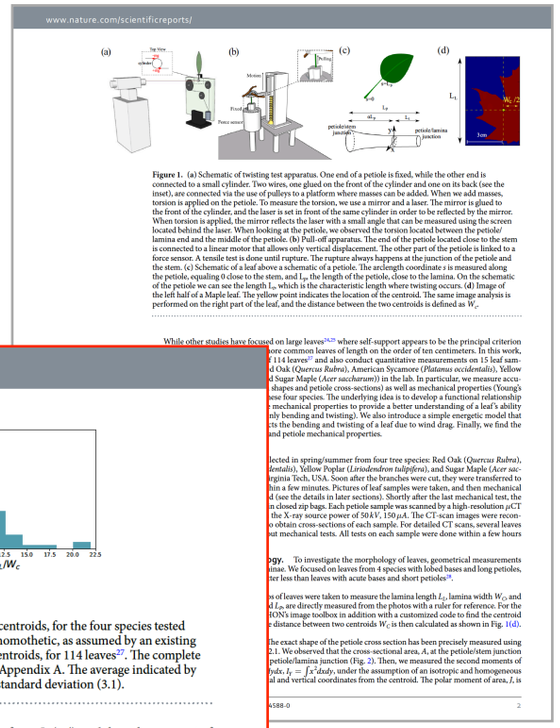

www.nature.com/scientificreports/

Figure 1. (a) Schematic of twisting test apparatus. One end of a petiole is fixed, while the other end is connected to a small cylinder. Two wires, one glued on the front of the cylinder and one on its back (see the inset), are connected via the use of pulleys to a platform where masses can be added. When we add masses, torsion is applied on the petiole. To measure the torsion, we use a mirror and a laser. The mirror is glued to the front of the cylinder, and the laser is set in front of the same cylinder in order to be reflected by the mirror. When torsion is applied, the mirror reflects the laser with a small angle that can be measured using the screen located behind the laser. When looking at the petiole, we observed the torsion located between the petiole/lamina end and the middle of the petiole. (b) Pull-off apparatus. The end of the petiole located close to the stem is connected to a linear motor that allows only vertical displacement. The other part of the petiole is linked to a force sensor. A tensile test is done until rupture. The rupture always happens at the junction of the petiole and the stem. (c) Schematic of a leaf above a schematic of a petiole. The arclength coordinate s is measured along the petiole, equaling 0 close to the stem, and L_p the length of the petiole, close to the lamina. On the schematic of the petiole we can see the length L_m which is the characteristic length where twisting occurs. (d) Image of the left half of a Maple leaf. The yellow point indicates the location of the centroid. The same image analysis is performed on the right part of the leaf, and the distance between the two centroids is defined as W_c.

While other studies have focused on large leaves[24,25] where self-support appears to be the principal criterion
ore common leaves of length on the order of ten centimeters. In this work,
f 114 leaves[27] and also conduct quantitative measurements on 15 leaf sam-
d Oak (*Quercus Rubra*), American Sycamore (*Platanus occidentalis*), Yellow
d Sugar Maple (*Acer saccharum*)) in the lab. In particular, we measure accu-
shapes and petiole cross-sections) as well as mechanical properties (Young's
ese four species. The underlying idea is to develop a functional relationship
mechanical properties to provide a better understanding of a leaf's ability
nly bending and twisting). We also introduce a simple energetic model that
cts the bending and twisting of a leaf due to wind drag. Finally, we find the
nd petiole mechanical properties.

lected in spring/summer from four tree species: Red Oak (*Quercus Rubra*),
dentalis), Yellow Poplar (*Liriodendron tulipifera*), and Sugar Maple (*Acer sac-*
rginia Tech, USA. Soon after the branches were cut, they were transferred to
hin a few minutes. Pictures of leaf samples were taken, and then mechanical
d (see the details in later sections). Shortly after the last mechanical test, the
n closed zip bags. Each petiole sample was scanned by a high-resolution μCT
the X-ray source power of 50 kV, 150 μA. The CT-scan images were recon-
o obtain cross-sections of each sample. For detailed CT scans, several leaves
ut mechanical tests. All tests on each sample were done within a few hours

ogy. To investigate the morphology of leaves, geometrical measurements
ime. We focused on leaves from 4 species with lobed bases and long petioles,
er less than leaves with acute bases and short petioles[28].

s of leaves were taken to measure the lamina length L_l, lamina width W_C, and
d L_P, are directly measured from the photos with a ruler for reference. For the
ON's image toolbox in addition with a customized code to find the centroid
e distance between two centroids W_C is then calculated as shown in Fig. 1(d).

The exact shape of the petiole cross section has been precisely measured using
2.1. We observed that the cross-sectional area, A, at the petiole/stem junction
petiole/lamina junction (Fig. 2). Then, we measured the second moments of
yda, $I_X = \int x^2 dady$, under the assumption of an isotropic and homogeneous
al and vertical coordinates from the centroid. The polar moment of area, J, is

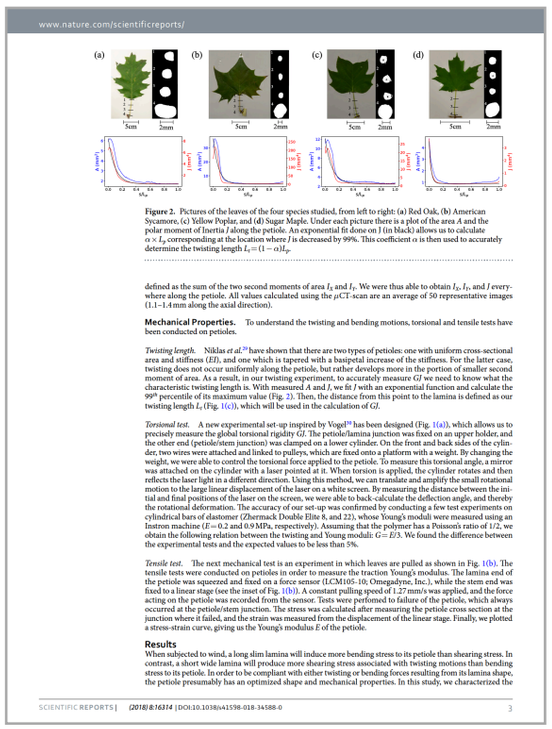

www.nature.com/scientificreports/

Figure 2. Pictures of the leaves of the four species studied, from left to right: (a) Red Oak, (b) American Sycamore, (c) Yellow Poplar, and (d) Sugar Maple. Under each picture there is a plot of the area A and the polar moment of Inertia J along the petiole. An exponential fit done on J (in black) allows us to calculate $\alpha \times L_p$ corresponding at the location where J is decreased by 99%. This coefficient α is then used to accurately determine the twisting length $L_t = (1-\alpha)L_p$.

defined as the sum of the two second moments of area I_L and I_T. We were thus able to obtain I_S, I_T, and J everywhere along the petiole. All values calculated using the μCT-scan are an average of 50 representative images (1.1–1.4 mm along the axial direction).

Mechanical Properties. To understand the twisting and bending motions, torsional and tensile tests have been conducted on petioles.

Twisting length. Niklas *et al.*[29] have shown that there are two types of petioles: one with uniform cross-sectional area and stiffness (EI), and one which is tapered with a basipetal increase of the stiffness. For the latter case, twisting does not occur uniformly along the petiole, but rather develops more in the portion of smaller second moment of area. As a result, in our twisting experiment, to accurately measure GJ we need to know what the characteristic twisting length is. With measured A and J, we fit J with an exponential (see Fig. 2). Then, the distance from this point to the lamina is defined as our twisting length L_t (Fig. 1(c)), which will be used in the calculation of GJ.

Torsional test. A new experimental set-up inspired by Vogel[30] has been designed (Fig. 1(a)), which allows us to precisely measure the global torsional rigidity GJ. The petiole/lamina junction was fixed on an upper holder, and the other end (petiole/stem junction) was clamped on a lower cylinder. On the front and back sides of the cylinder, two wires were attached and linked to pulleys, which are fixed onto a platform with a weight. By changing the weight, we were able to control the torsional force applied to the petiole. To measure this torsional angle, a mirror was attached on the cylinder with a laser pointed at it. When torsion is applied, the cylinder rotates and then reflects the laser light in a different direction. Using this method, we can translate and amplify the small rotational motion to the large linear displacement of the laser on a white screen. By measuring the distance between the initial and final positions of the laser on the screen, we were able to back-calculate the deflection angle, and thereby the rotational deformation. The accuracy of our set-up was confirmed by conducting a few test experiments on cylindrical bars of elastomer (Zhermack Double Elite 8, and 22), whose Young's moduli were measured using an Instron machine ($E = 0.2$ and 0.9 MPa, respectively). Assuming that the polymer has a Poisson's ratio of 1/2, we obtain the following relation between the twisting and Young moduli: $G = E/3$. We found the difference between the experimental tests and the expected values to be less than 5%.

Tensile test. The next mechanical test is an experiment in which leaves are pulled as shown in Fig. 1(b). The tensile tests were conducted on petioles in order to measure the traction Young's modulus. The lamina end of the petiole was squeezed and fixed on a force sensor (LCM105-10, Omegadyne, Inc.), while the stem end was fixed to a linear stage (see the inset of Fig. 1(b)). A constant pulling speed of 1.27 mm/s was applied, and the force acting on the petiole was recorded from the sensor. Tests were performed to failure of the petiole, which always occurred at the petiole/stem junction. The stress was calculated after measuring the petiole cross section at the junction where it failed, and the strain was measured from the displacement of the linear stage. Finally, we plotted a stress-strain curve, giving us the Young's modulus E of the petiole.

Results

When subjected to wind, a long slim lamina will induce more bending stress to its petiole than shearing stress. In contrast, a short wide lamina will produce more shearing stress associated with twisting motions than bending stress to its petiole. In order to be compliant with either twisting or bending forces resulting from its lamina shape, the petiole presumably has an optimized shape and mechanical properties. In this study, we characterized the

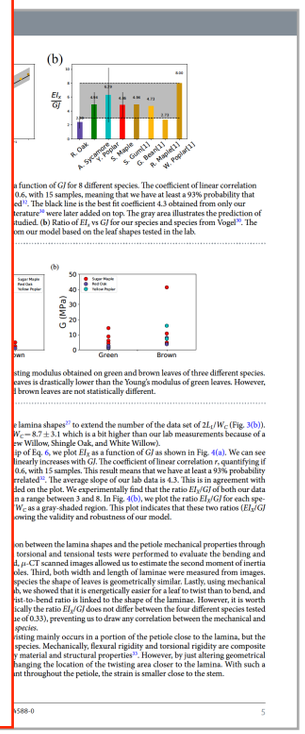

(b)

function of GJ for 8 different species. The coefficient of linear correlation
0.6, with 15 samples, meaning that we have at least a 93% probability that
ed[31]. The black line is the best fit coefficient 4.3 obtained from only our
erature[29] were later added on top. The gray area illustrates the prediction of
studied. (b) Ratio of EI_X vs GJ for our species and species from Vogel[30]. The
om our model based on the leaf shapes tested in the lab.

(b)

sting modulus obtained on green and brown leaves of three different species.
eaves is drastically lower than the Young's modulus of green leaves. However,
brown leaves are not statistically different.

e lamina shapes[27] to extend the number of the data set of $2L_l/W_C$ (Fig. 3(b)),
$W_C = 8.7 \pm 3.1$ which is a bit higher than our lab measurements because of a
ew Willow, Shingle Oak, and White Willow).
ip of Eq. 6, we plot EI_X as a function of GJ as shown in Fig. 4(a). We can see
linearly increases with GJ. The coefficient of linear correlation r, quantifying if
0.6, with 15 samples. This result means that we have at least a 93% probability
rrelated[32]. The average slope of our lab data is 4.3. This is in agreement with
ded on the plot. We experimentally find that the ratio EI_X/GJ of both our data
n a range between 3 and 8. In Fig. 4(b), we plot the ratio EI_X/GJ for each spe-
W_C as a gray-shaded region. This plot indicates that these two ratios (EI_X/GJ
owing the validity and robustness of our model.

on between the lamina shapes and the petiole mechanical properties through
torsional and tensional tests were performed to evaluate the bending and
L μ-CT scanned images allowed us to estimate the second moment of inertia
oles. Third, both width and length of laminae were measured from images.
species the shape of leaves is geometrically similar. Lastly, using mechanical
h, we showed that it is energetically easier for a leaf to twist than to bend, and
ist-to-bend ratio is linked to the shape of the laminae. However, it is worth
ically the ratio EI_X/GJ does not differ between the four different species tested
ze of 0.33), preventing us to draw any correlation between the mechanical and
species.
isting mainly occurs in a portion of the petiole close to the lamina, but the
species. Mechanically, flexural rigidity and torsional rigidity are composite
y material and structural properties[30]. However, by just altering geometrical
hanging the location of the twisting area closer to the lamina. With such a
nt throughout the petiole, the strain is smaller close to the stem.

www.nature.com/scientificreports/

Our simple model is based on wind-induced bending and twisting stress, yet we are not able to capture the detailed dynamics of leaf motions. In particular, we are aware that in nature the bending and twisting of leaves are not static, but more dynamic (e.g. fluttering). While we focused on torsion and traction tests, our approach can also be extended with bending measurements to some extent.

Our samples were collected during spring/summer when trees grow their leaves and produce food through photosynthesis. However, leaves in the fall might exhibit different mechanical properties as trees are inclined to lose their leaves. We conducted exploratory tests in Fall 2016 on the same trees. We found a drastic decrease in the Young's modulus (351 ± 303 MPa for green leaves and 68 ± 39 MPa for brown leaves), but not in the twisting modulus (4.1 ± 3.8 MPa for green leaves and 12.1 ± 11.7 MPa for brown leaves), as shown in Fig. 5. However, mechanical testings were difficult to perform, as leaves twisted-off very easily. Therefore, to conclude on this trend, we need more measurements.

References

1. El-Sharkawy, M. & Hesketh, J. Photosynthesis among species in relation to characteristics of leaf anatomy and co2 diffusion resistances. *Crop. Sci.* **5**, 517–521 (1965).
2. Vogel, S. The life of a leaf (University of Chicago Press, Chicago, 2012).
3. Tadrist, L., Saudreau, M. & de Langre, E. Wind and gravity mechanical effects on leaf inclination angles. *J. Theor. Biol.* **341**, 9–16 (2014).
4. Niklas, K. J. Plant Allometry (University of Chicago Press, 1994).
5. Niklas, K. Plant biomechanics: an engineering approach to plant form and function (The University of Chicago Press, 1992).
6. Nänsemets, Ü. & Fleck, S. Petiole mechanics, leaf inclination, morphology, and investment in support in relation to light availability in the canopy of liriodendron tulipifera. *Oecologia* **132**, 21–33 (2002).
7. Roden, J. S. & Pearcy, R. W. Effect of leaf flutter on the light environment of poplars. *Oecologia* **93**, 201–207 (1993).
8. Takenaka, A. Effects of leaf blade narrowness and petiole length on the light capture efficiency of a shoot. *Ecol. Res.* **9**, 109–114 (1994).
9. Roden, J. S. Modeling the light interception and carbon gain of individual fluttering aspen (populus tremuloides michx) leaves. *Trees* **17**, 117–126 (2003).
10. Vogel, S. Leaves in the lowest and highest winds: temperature, force and shape. *New Phytol.* **183**, 13–26 (2009).
11. Anten, N. P. R., Alcalá-Herrera, R., Schieving, F. & Onoda, Y. Wind and mechanical stimuli differentially affect leaf traits in plantago major. *New Phytol.* **188**, 554–564 (2010).
12. de Langre, E. Effects of wind on plants. *Annu. Rev. Fluid Mech.* **40**, 141–168 (2008).
13. Jensen, K. H. & Zwieniecki, M. A. Physical limits to leaf size in tall trees. *Phys. Rev. Lett.* **110**, 018104 (2013).
14. Poorter, H. & Nagel, O. The role of biomass allocation in the growth response of plants to different levels of light, co2, nutrients and water: a quantitative review. *Aust. J. Plant Physiol.* **27**, 595–607 (2000).
15. Niklas, K. J. Biomechanical responses of chamaedorea and spathiphyllum petioles to tissue dehydration. *Annals Bot.* **67**, 67–76 (1991).
16. Duan, S. *et al.* The global spectrum of plant form and function. *Nat.* **529**, 167–171 (2015).
17. Jaffe, M. J. T. The response of plant growth and development to mechanical stimulation. *Planta* **114**, 143–157 (1973).
18. Knight, T. A. Account of some experiments on the descent of sap in trees. Philos. *Transactions Royal Soc. Lond.* **93**, 277–289 (1803).
19. Jacobs, M. R. The effect of wind sway on the form and development of pinus radiata d. don. *Aust. J. Bot.* **2**(2), 35–51 (1954).
20. Coutand, C. Biomechanical study of the effect of a controlled bending on tomato stem elongation: global mechanical analysis. *J. Exp. Bot.* **51**, 1813–1824 (2000).
21. Loué, L., Guerra, G., Badel, E. & Forterre, Y. A universal mechanism for hydraulic signals generation in biomimetic and natural branches. *Proc. Natl. Acad. Sci.* **114**, 11034–11039 (2017).
22. Niklas, K. J. The elastic moduli and mechanics of populus tremuloides (salicaceae) petioles in bending and torsion. *Am. J. Bot.* **78**, 989–996 (1991).
23. Niklas, K. J. Differences between acer saccharum leaves from open and wind-protected sites. *Annals Bot.* **78**, 61–66 (1996).
24. Ennos, A. R., Spatz, H. & Speck, T. The functional morphology of the petioles of the banana, Musa textilis. *J. Exp. Bot.* **51**, 2085–2093 (2000).
25. Hejnowicz, Z. & Barthlott, W. Structural and mechanical peculiarities of the petioles of giant leaves of amorphophallus (araceae). *Ann. J. Bot.* **92**, 391–403 (2005).
26. Tadrist, L. & Derbois-Texier, B. Are leaves optimally designed for self-support? an investigation on giant monocots. *J. Theor. Biol.* **396**, 125–131 (2016).
27. Chang, Y. W. *et al.* Leafesap: An electronic field guide (2011).
28. Vogel, S. Drag and reconfiguration of broad leaves in high winds. *J. Exp. Bot.* **40**, 941–948 (1989).
29. Niklas, K. J. Flexural stiffness allometries of angiosperm and fern petioles and rachises: evidences for biomechanical convergence. *Evol.* **45**, 734–750 (1991).
30. Vogel, S. Twist-to-bend ratios and cross-sectional shapes of petioles and stems. *J. Exp. Bot.* **43**, 1527–1532 (1992).
31. Monsi, M. & Saeki, T. On the factor light in plant communities and its importance for matter production. *Annals Bot.* **95**, 549–567 (2005).
32. Taylor, J. R. An Introduction to Error Analysis (University Science Books, 1982).
33. Wainwright, S. A., Biggs, W. D., Currey, J. D. & Gosline, J. M. Mechanical Design in Organism (Princeton University Press, Princeton, 1976).
34. Tuselli, P. & Bockstal, J. Imaging Spectroscopy: Fundamentals and Prospective Applications (Kluwer Academic Publishers, 1991).

Acknowledgements

This research was supported by National Science Foundation Grant CBET-1604424. Hosung Kang was supported by the Postdoctoral Research Program of Sungkyunkwan University (2015).

Author Contributions

J.-F.L., P.N.S., T.Z. and S.J. designed research; J.-F.L., L.N., H.K., P.N.S., T.Z. and S.J. performed research; J.-F.L., L.N., P.N.S., T.Z. and S.J. analyzed data; and J-F.L., T.Z. and S.J. wrote the paper.

Additional Information

Supplementary information accompanies this paper at https://doi.org/10.1038/s41598-018-34588-0.

Competing Interests: The authors declare no competing interests.

Step 3: Use Microsoft PowerPoint, Microsoft Excel, Apple Keynote, Apple Numbers or Adobe Photoshop to create your figure or table.

	2009	2010	2011	2012	2013	2014	2015	2016	2017	2018
American Sycamore	131	136	134	140	142	146	148	146	150	152
Red Maple	123	120	104	100	95	80	63	55	51	50
Tulip Poplar	235	238	243	269	288	312	342	373	403	433
White Oak	429	415	401	365	322	286	222	150	73	51
Total	918	909	882	874	847	824	775	724	677	686

This table is from the Louf et al., 2018 journal article. The table is fine but I think my audience would better understand these data as a colorful graph for my poster. So I decided to use Apple Numbers (I could have also used Microsoft Excel) to create a graph from these data. This graph is my original figure that I will add to my poster.

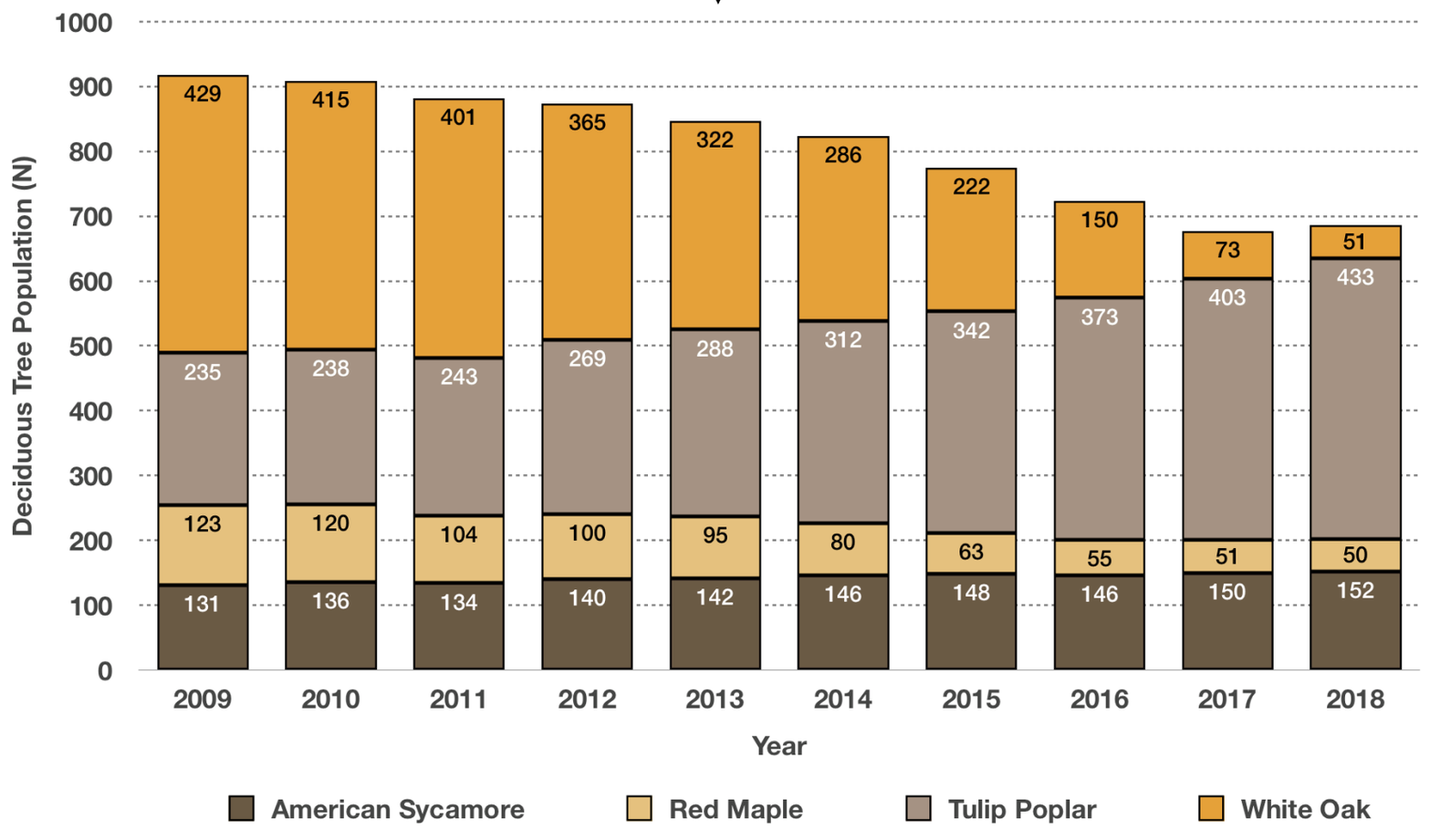

Step 4: Write a figure caption (in your own words) to accompany the figure on your poster. And remember to cite the source(s) of your information in the caption.

Do NOT copy/paste your figure caption from the journal article. You should write the caption in your own words. This demonstrates to Dr. Lower (and your audience) that you truly understand the data contained within the graph.

Figure Caption: Population of American Sycamore, Red Maple, Tulip Poplar and White Oak in Glacier Peak National Park from 2009-2018. American Sycamore shown in brown, Red Maple in light orange, Tulip Poplar in tan and White Oak in dark orange. **Data obtained from Louf, Nelson, Kang, Song, Zehnbauer and Jung (2018), Scientific Reports, 8:16314.**

ALWAYS remember to cite your sources in your figure captions

Step 5: Insert the figure into my poster. Below is my finished figure (Figure X) and figure caption that I will insert in my poster.

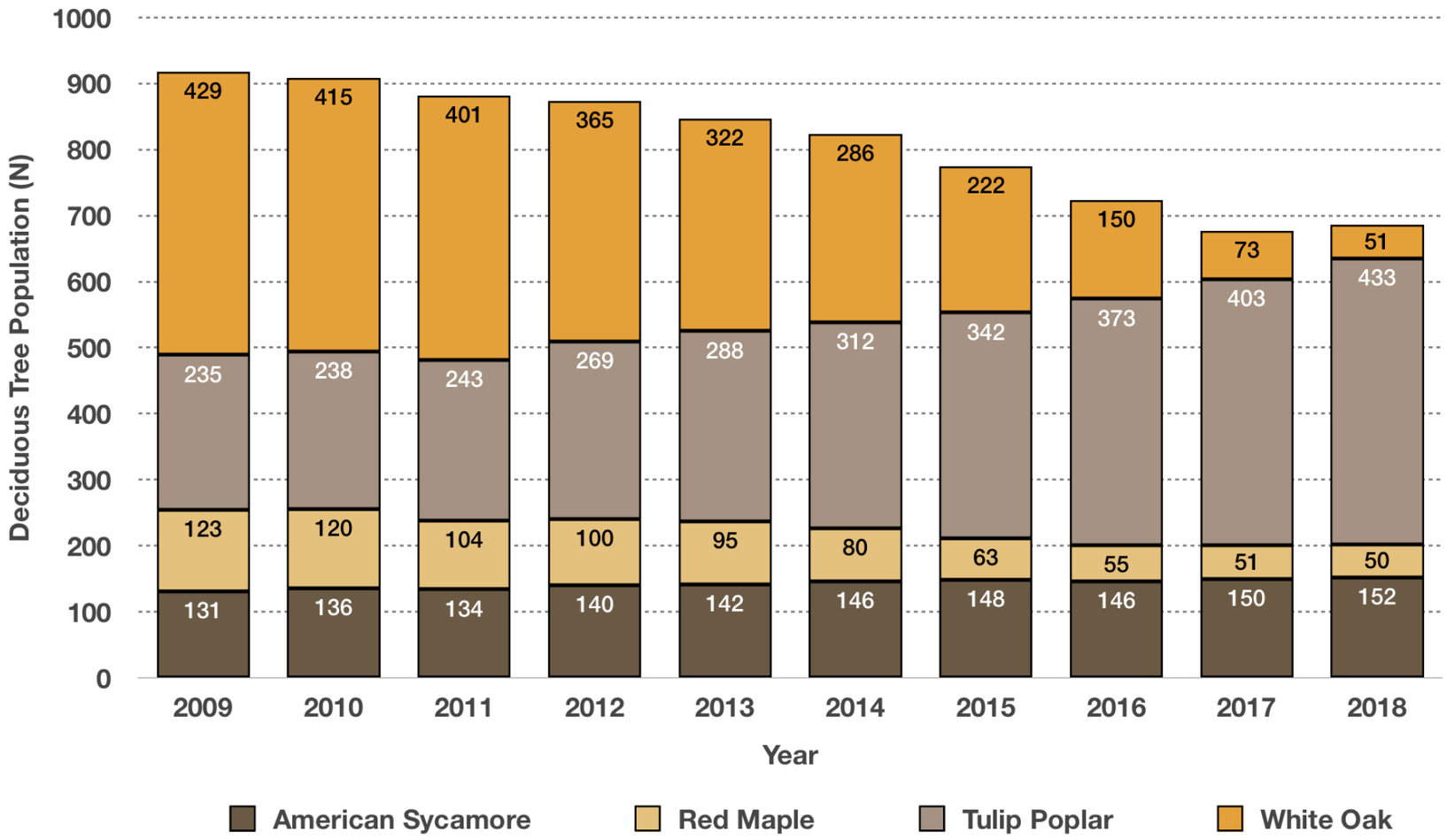

Figure X: Population of American Sycamore, Red Maple, Tulip Poplar and White Oak in Glacier Peak National Park from 2009-2018. American Sycamore shown in brown, Red Maple in light orange, Tulip Poplar in tan and White Oak in dark orange. Data obtained from Louf, Nelson, Kang, Song, Zehnbauer and Jung (2018), Scientific Reports, 8:16314.

Glacier Peak National Park, Impact and Treatment Plans for Deciduous Trees Infected by the Blue Spotted Yellow Hopper

Brian H. Lower, The Ohio State University, School of Environment & Natural Resources

48-inches

36-inches

ABSTRACT

This editable template is a common poster size (48" x 36") and orientation (horizontal); and will be the size of poster that will be used for the class and to print (if in the in person section of the course).

Writing Style:

The writing style for scientific posters should match the guidelines for the university. Use the Editorial Style Guide at **osu.edu/brand** for general guidance with academic titles, names of campus buildings, the correct way to refer to the campus, etc.

Copyright and Intellectual Property Guidelines

In today's world, just about everything is copyrighted whether it carries the copyright symbol© or not. Under today's law, materials are protected by copyright as soon as they are completed. Copyright applies broadly to all creative pieces, stone, found in cyt more information, or send an email t

INTRODUCTION

How to use this template:

Highlight this text and replace it with new text from a Microsoft Word document or other text-editing program. The text size for body copy and headings and the typeface has been set for you. The text boxes and photo boxes may be resized, eliminated, or added as necessary. The references to the department, college and university, including the logo, should remain.

Header, to label the table below

small copylm ipit, quam aliquis nullan volobor am quat vulla faci bla feuisl ea facidunt luptatin ut prat. Henim do conse feum nim velessim nulla augiat, quat acil ulla acin henim irit alit praesto commod te doloborperos acilla facincin henit lan henim ilit atincil laortisl enit praestie molore feugiam ver in eummy nos dolortisi bla faci

METHODS

Text

Be sure to spell check all text and have trusted colleagues proofread the poster. In general, authors should:

Authors should re-write their paper so that it is suitable for the brevity of the poster format. Respect your audience. As a general rule, less is more. Use a generous amount of white space to separate elements and avoid data overkill. Refer to Web sites or other sources to provide a more in- depth understanding of the research.

Header, to label the table below

small copylm ipit, quam aliquis nullan volobor am quat vulla faci bla feuisl ea facidunt luptatin ut prat. Henim do conse feum nim velessim nulla augiat, quat acil ulla acin henim irit alit praesto commod te doloborperos acilla facincin henit lan henim ilit atincil laortisl enit praestie molore feugiam ver in eummy nos dolortisi bla faci Rit dolesendus, tet endenis ea volupta eperere ssenem nam hictus.

RESULTS

Images

Images must be 72 to 100 dpi in their final size, or use a rule of thumb of 2 to 4 megabytes of uncompressed .tif file per square foot of image. For instance, a 3x5 photo that will be

Header, to label the table below

I inserted Figure 5 and Figure 5 caption in the Results section (column 3) of my poster.

Figure 5 Graph

Figure 5 Caption

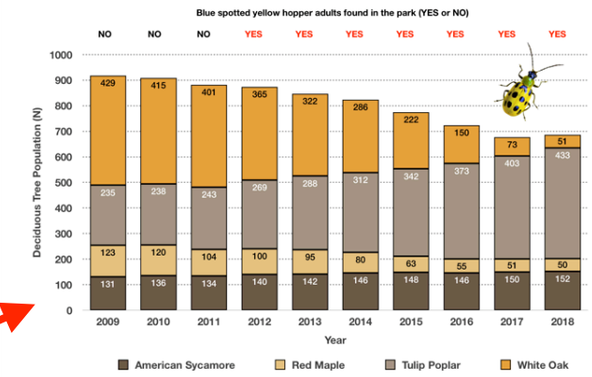

Figure 5. Population of American Sycamore, Red Maple, Tulip Poplar and White Oak in Glacier Peak National Park from 2009-2018. American Sycamore shown in brown, Red Maple in light orange, Tulip Poplar in tan and White Oak in dark orange. An adult blue spotted yellow hopper is shown at the top right. Individual adult insects were captured within the park using a Browns-Oats Insect Trap baited with lepidopteran pheromone. "NO" indicates that no insects were captured in the park, "YES" indicates that insects were captured in the park. Data obtained from Louf, Nelson, Kang, Song, Zehnbauer and Jung (2018), Scientific Reports, 8:16314. Image obtained from U.S. Department of Agriculture, Pest Insects Technical Report (2016), Chicago, Illinois, pp. 182-184.

DISCUSSION

We have created this template with scientific researchers in mind. We encourage any comments or suggestions so that we can continue to update and improve this template.
E-mail **identity@osu.edu** with suggestions.

REFERENCES

1. References. lum exer adipsustrud doloree tuerat lorpera esenibh eu faccum eum iuscili quamcommy nit lorerillut ullam quat lore verostrud ming et, si tie faciliquisse modolortin volore
2. vel et vel dionsenit adit, consenim zzrillute el euguerostie faci bla conse minim zzriure tio dolore tet, volobor si.
3. Velit vendipit, quat iustrud eraeseniat do conummod ea alisci tie vel ea commodo lortis aliquamcommy niat aliquat niam ercillan eu feugue magnisl utpat autat.
4. Ut nostionsed molobore feugiam quiscing exeraese ting etue dit atetum ipsum inim ex exercin cincincinci et lut incinis er in
5. henibh esequat, quis aci eniamet ut ad modolutpat wis eumsandipit aliquipsum zzriure verosto enim ea feu faccum vulputet vel utet non ute conse tis dip er aliquam cortin henim duipisim iuscing ex et nos dolorem zzrit wiscilit er sisl.
6. Sim ipsum dolorem velis aut vulputpat eu facilit am delestrud eui blan vendre elisisc illaorp ercilisi blan eu faccumsandre tat dipit nis dionull amconsequa.
7. Source 7
8. Source 8
9. Source 9
10. Source 10

Printing your Poster

There is a handful of cost-effective places with poster printing capabilities at the university. Plan ahead as one poster can take 30 minutes or longer to print.

We recommend printing your poster at UniPrint at the Ohio Union. You will receive a discount of $36 for the course.

Repeat Steps 1-5 for the rest of my figures and tables. In the example Poster Outline below you can see that my final poster will have 5 figures and 1 table.

Figure 3. Photograph of an insect trap that was used by the scientists to trap the insects in the park. Also include a photograph showing the scientists looking at the insects under the microscope.

Figure 5. Graph showing the population of trees in Glacier Peak National Park over the past 10 years. Show numbers for each of the 4 trees that the scientists studied and show when the blue spotted yellow hopper insect was detected in the park.

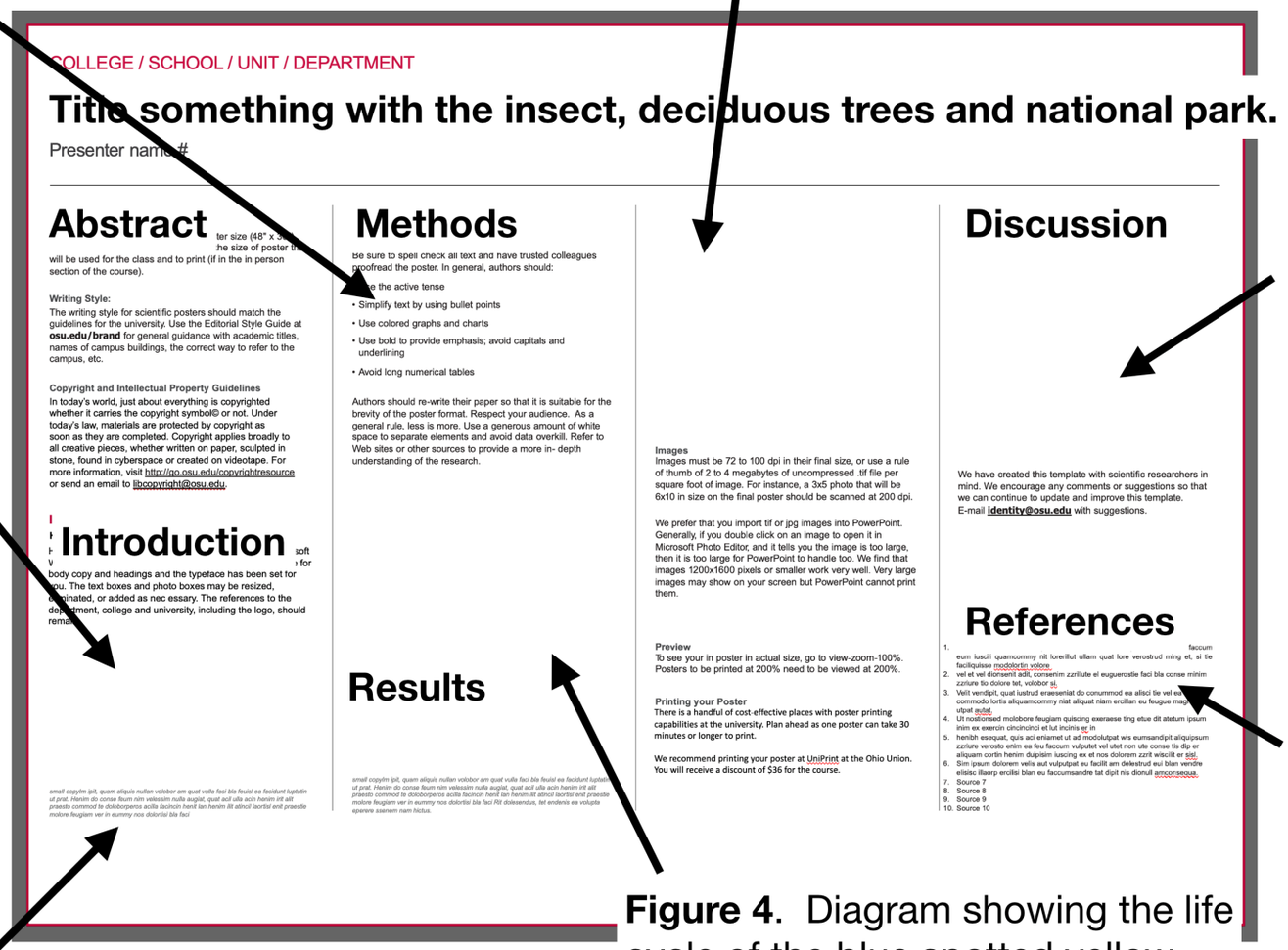

Figure 1. Map of Glacier Peak National Park, map showing location of park in USA. Map will be satellite image. Also include photograph of the park itself showing what an ecosystem looks like at the park.

Table 1. Show the different types of insecticides that the scientist used to kill the insect and how effective each chemical was at killing the insect.

Provide my **references** here, numbered 1-15. I know I only needed 10, but I actually found an additional 5 references that I used in my poster.

Figure 2. 4 photographs of the deciduous trees included in the study (red maple, white oak, American sycamore, Tulip popular. 1 photograph of an adult blue spotted yellow hopper

Figure 4. Diagram showing the life cycle of the blue spotted yellow hopper (egg, larvae, pupae, adult) and where each lives in forest. And how it infects and kills trees.